High Chern number quantum anomalous Hall phases in single-layer graphene with Haldane orbital coupling

Tsung-Wei Chen,[1,2,*] Zhi-Ren Xiao,[3] Dah-Wei Chiou,[1,4] and Guang-Yu Guo[1,3,†]

[1]*Department of Physics and Center for Theoretical Sciences, National Taiwan University, Taipei 106, Taiwan*
[2]*Department of Physics, National Sun Yat-sen University, Kaohsiung 804, Taiwan*
[3]*Graduate Institute of Applied Physics, National Chengchi University, Taipei 116, Taiwan*
[4]*Center for Condensed Matter Sciences, National Taiwan University, Taipei 106, Taiwan*

We investigate possible phase transitions among the different quantum anomalous Hall (QAH) phases in single-layer graphene under the influence of the exchange field. The effective tight-binding Hamiltonian for graphene is made up of the hopping term, the Kane-Mele and Rashba spin-orbit couplings as well as the Haldane orbital term. We find that the variation of the exchange field results in bulk gap-closing phenomena and phase transitions occur in the graphene system. If the Haldane orbital coupling is absent, the phase transition between the chiral (antichiral) edge state $\nu = +2$ ($\nu = -2$) and the pseudoquantum spin Hall state ($\nu = 0$) takes place. Surprisingly, when the Haldane orbital coupling is taken into account, an intermediate QSH phase with two additional edge modes appears in between phases $\nu = +2$ and $\nu = -2$. This intermediate phase is therefore either the hyperchiral edge state of high Chern number $\nu = +4$ or antihyperchiral edge state of $\nu = -4$ when the direction of exchange field is reversed. We present the band structures, edge state wave functions, and current distributions of the different QAH phases in the system. We also report the critical exchange field values for the QAH phase transitions.

I. INTRODUCTION

The anomalous integer quantum Hall effect observed in monolayer graphene subjected to an external magnetic field[1,2] has recently attracted considerable attention. A theoretical investigation[3] showed that plateaus located at the half-odd-integer position originate from an additional Landau level at zero energy,[4,5] which is unlike the behavior of the conventional quantum Hall effect observed in two-dimensional (2D) heterostructure semiconductors.[6] The quantum Hall effect has also been experimentally observed in AB-stacked bilayer graphene,[7] and this has been studied theoretically as well.[8,9] Furthermore, much experimental evidence is available for the existence of AA-stacked bilayer graphene.[10] Interestingly, AA-stacked bilayer graphene has been shown to exhibit zero transverse conductivity.[11]

According to Laughlin's gauge invariance argument, the sample edges are essential in generating the localized current-carrying states (edge states).[12,13] The edge states on the sample boundary are protected by the bulk band structure topology, which is a manifestation of the Chern number, as elucidated by Thouless *et al.* (TKNN).[14] The TKNN integer ν (or Chern number) relates the topological class of the bulk band structure to the number of chiral edge states on the sample boundary (bulk-boundary correspondence) and hence gives rise to the quantized Hall conductivity $\sigma_{xy} = \nu\, e^2/h$. The precise quantization of the Hall conductivity arises in the 2D electron system with an integer filling of the Landau levels. The Chern number corresponding to the number of the chiral edge currents equals to the number of Landau levels below the Fermi level. When the system undergoes a phase transition from one chiral edge state to another, the corresponding Chern number varies discontinuously from one integer ν to $\nu \pm 1$.

The Chern number must vanish in a system with time reversal symmetry (TRS). A TRS breaking mechanism is thus required for a 2D system to achieve a nonzero Chern number, either with or without the Landau levels. It has been shown that the chiral edge state in the quantum Hall phase is related to the parity anomaly of 2D Dirac fermions.[15,16] Therefore, in a remarkable paper,[17] Haldane constructed a tight-binding Hamiltonian in the 2D honeycomb lattice with a staggered magnetic field that produces zero average magnetic flux per unit cell (i.e., no Landau levels), and showed that the gapped state exhibits the quantum Hall phase with $\nu = \pm 1$. In this sense, the Haldane model is the prototype for the quantum anomalous Hall (QAH) effect. The relationship between the Chern number and the winding number of the edge state was investigated in Ref. 18.

On the other hand, when the bulk band gap of a system having a spin degree of freedom is opened due to the spin-orbit interaction, the system might be in the quantum spin Hall (QSH) state where the gapless edge states appearing on the sample boundary are protected by the TRS.[19] The quantization of the spin Hall conductivity has been predicted in a graphene system with the Kane-Mele spin-orbit interaction as well as in a semiconductor superlattice.[20–22] The quantization of the spin Hall conductivity, however, may be destroyed by the parity-breaking perturbations via spin nonconserving term or disorder. The associated topological invariant classifying the band structure topology of the time-reversal invariant systems is a Z_2 topological index.[20,21] The connection between the Chern number and the Z_2 topological index is explained in Ref. 23. The Z_2 topological number represents the number of the Kramer pairs of the gapless edge modes. An important result of this classification is that these gapless edge modes with an odd number of the Kramer pairs in the 2D systems[20–22] and an odd number of surface Dirac cones in the three-dimensional

(3D) systems[24,25] are robust to impurity scattering; the other systems are just a conventional band insulator.

Recently, another topological invariant (i.e., the spin Chern number) has been proposed by Sheng *et al.*,[26] and it can be evaluated by imposing twisted boundary conditions on a finite sample. In Ref. 27, it has been shown that the spin Chern number and Z_2 topological orders would yield the same classification by investigating the bulk gap-closing phenomena in the time-reversal invariant systems. The phase diagram of the 3D QSH systems has been investigated systematically.[28] The topological winding number related to the spin edge states of graphene with the Kane-Mele Hamiltonian has also been studied.[29] Furthermore, the bulk-boundary correspondence is generalized to classify topological defects in insulators and superconductors, where the gapless boundary excitations are Majorana fermions.[30]

In this paper, we first model the bulk graphene and also a zigzag graphene ribbon in the presence of the exchange field[31] by using the Kane-Mele-Rashba Hamiltonian [see Eq. (1)]. Here, the spin degeneracy is lifted by the TRS breaking term (i.e., the exchange field) and the $z \to -z$ mirror symmetry is broken by the Rashba term. We calculate the Chern number of the bulk system as a function of the exchange field strength. Furthermore, we study how the edge current in the corresponding graphene ribbon varies during a phase transition induced by the exchange field.

The quantum anomalous Hall effect in $Hg_{1-y}Mn_yTe$ quantum wells[32] and tetradymite semiconductors (Bi_2Te_3, Bi_2Se_3, and Sb_2Te_3)[33] has been investigated. Graphene with the Rashba spin-orbit coupling [α, see Eq. (2c)] and the exchange field has also been studied before.[34] However, in Ref. 34, the Kane-Mele spin-orbit coupling [λ, see Eq. (2b)] was neglected because it was thought to be weaker than the Rashba spin-orbit interaction. In this paper, we find that, in the presence of both the Rashba and Kane-Mele couplings, a phase transition from either a chiral ($\nu = +2$) or antichiral ($\nu = -2$) edge state ($\nu = \pm 2$) to the pseudo-QSH state ($\nu = 0$) would occur in graphene, because of the change of the Chern number due to the bulk gap-closing phenomena. This phase transition is different from the transition between the QSH state and the insulator state when the exchange field is absent.

We then add the Haldane orbital coupling term, which couples the electron orbital motion to the exchange field[17] to the Kane-Mele-Rashba Hamiltonian for graphene. Interestingly, we find that this leads to an anomalous change in the Chern number pattern. Note that the Haldane orbital term does not lift the spin degeneracy. Furthermore, we find that the presence of the Haldane orbital coupling would give rise to a new intermediate phase between phases $\nu = +2$ and $\nu = -2$. This intermediate phase has two new edge modes, and is thus either a hyperchiral edge state with $\nu = +4$ or an antihyper chiral edge state with $\nu = -4$ when the direction of the exchange field is reversed.

The rest of this paper is organized as follows. In Sec. II, we describe the effective tight-binding Hamiltonian for graphene used in this work. In Sec. III, we report the energy bands of a graphene ribbon in the presence of the exchange field. In Sec. IV, we present the phase transition and the variation of the Chern number with the exchange field in the Kane-Mele-Rashba system. In particular, we show that graphene undergoes a phase transition from the chiral (or antichiral) state to the pseudo-QSH state. In Sec. V, we show that a hyperchiral (or antihyperchiral) state would appear in between the chiral and antichiral states in the Haldane-Rashba system. The conclusions are given in Sec. VI. The pseudo-QSH state is explained in Appendix A. The edge states and the variation of Chern number for smaller values of Kane-Mele and Rashba couplings are also discussed in Appendix B.

II. EFFECTIVE TIGHT-BINDING HAMILTONIAN FOR GRAPHENE

We consider the effective tight-binding model for graphene given by the Kane-Mele-Rashba Hamiltonian:[20,21]

$$H_{KMR} = H_t + H_\lambda + H_\alpha, \tag{1}$$

with

$$H_t = t \sum_{\langle i,j \rangle} c_i^\dagger c_j, \tag{2a}$$

$$H_\lambda = i\lambda \sum_{\langle\langle i,j \rangle\rangle} c_i^\dagger s_z v_{ij}^z c_j, \tag{2b}$$

$$H_\alpha = i\alpha \sum_{\langle i,j \rangle} c_i^\dagger (\mathbf{s} \times \mathbf{d}_{ij})_z c_j. \tag{2c}$$

The symbols $\langle i,j \rangle$ and $\langle\langle i,j \rangle\rangle$ denote the nearest and the next-nearest neighbors, respectively. The Hamiltonian H_t is the tight-binding energy for the nearest-neighbor hopping. The Kane-Mele Hamiltonian H_λ describes the intrinsic spin-orbit interaction. The opened band gap via Kane-Mele coupling determined by theoretical calculations ranges from 0.001 to 0.05 meV.[35] However, the Kane-Mele coupling is theoretically found to be significantly enhanced by impurity-induced sp^3 distortion of the flat graphene[36] and two mechanisms via hydrogenated and fluorinated graphene.[37] The site-dependent Haldane phase factor[17] v_{ij} is defined as

$$v_{ij} = \frac{\mathbf{d}_1 \times \mathbf{d}_2}{|\mathbf{d}_1 \times \mathbf{d}_2|}, \tag{3}$$

where $\mathbf{d}_i$ denotes the vector from one carbon atom to one of its nearest neighbors. Two vectors $\mathbf{d}_1$ and $\mathbf{d}_2$ are required to represent the second neighbor hopping (see Fig. 1). In the two-dimensional case, the nonzero component v_{ij}^z becomes a sign function, and we take the values of ± 1 (i.e., counterclockwise/clockwise). The extrinsic spin-orbit interaction is described by the Rashba Hamiltonian H_α, which can be produced by, e.g., applying an electric field $\mathbf{E}$ perpendicular to the graphene sheet. H_α is proportional to $\mathbf{E} \cdot (\mathbf{s} \times \mathbf{d}_{ij})$, where $\mathbf{E} = E_z \hat{e}_z$ and $\mathbf{d}_{ij}$ denotes the vector from site i to site j (see Fig. 1). The Rashba coupling is experimentally proved to be very large for graphene grown on the substrate.[38,39] The largest energy shift is 225 meV.[39]

Recently, it has been shown that graphene at low doping can stabilize a ferromagnetic phase via exchange interactions between Dirac fermions.[40] Recent *ab initio* density functional calculations also showed that intrinsic ferromagnetism in pure and on-top-Fe-doped graphene monolayers may exist.[34] Furthermore, proximity-[41] and defect-induced[42] ferromagnetism in graphene have also been reported.[43] Therefore we consider
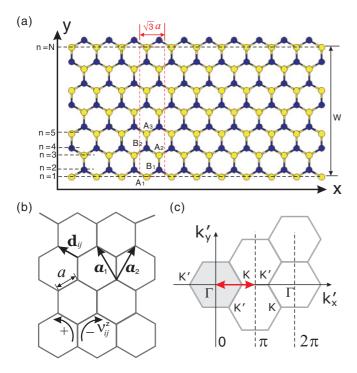
FIG. 1. (Color online) (a) A segment of a zigzag graphene ribbon with its unit cell marked by the red dashed lines. (b) Illustrations of Haldane phase factors v_{ij}^z, vectors $\mathbf{d}_{ij}$, bulk basis vectors $(\boldsymbol{a}_1, \boldsymbol{a}_2)$, and bond length a. (c) The first Brillouin zones of bulk graphene (gray region) and the zigzag graphene ribbon (red double arrow) in the 2D k space.

the interaction of the 2D electrons in graphene with the exchange field produced by the ferromagnetism.[31]

The coupling of the orbital motion and also spin of the electrons on graphene to the exchange field would give rise to an additional Hamiltonian:

$$H_{ex} = H_\gamma + H_\beta, \qquad (4)$$

with

$$H_\gamma = \gamma \sum_i c_i^\dagger s_z c_i, \qquad (5a)$$

$$H_\beta = i\tilde{\beta}(\gamma') \sum_{\langle\langle i,j \rangle\rangle} c_i^\dagger v_{ij}^z c_j, \qquad (5b)$$

where γ is the (rescaled) exchange-field strength. The coupling γ is proportional to $J_{eff}\mu_z'$, where J_{eff} is the exchange interaction and μ_z' is the effective magnetic moment associated with the exchange field. The magnetic field generated by μ_z' is denoted as γ'. The Hamiltonian H_γ describes the response of an electron spin magnetic moment to the exchange field *à la* Zeeman effect.

In the meantime, the orbital angular momentum of an electron in graphene would be coupled to the exchange field because of its associated orbital magnetic moment. The Haldane phase factor $\boldsymbol{v}_{ij}$ behaves like an effective orbital angular momentum, and hence gives rise to the interaction between the electron orbital motion and the magnetic field γ', as described by Eq. (5b), where $\tilde{\beta}(\gamma')$ is a function of γ'. Spatial parity symmetry requires $\tilde{\beta}(\gamma')$ to be an odd function of γ'. Unlike the interaction between the spin and exchange field,

the energy of the Haldane orbital coupling cannot be linear in the exchange filed γ'. Instead, the response of Haldane orbital motion would be saturated rapidly because the exchange field γ' alters the orbital velocity of electrons and induces an orbital magnetic moment against it. Phenomenologically, we can adopt the simple yet sensible approximation:

$$\tilde{\beta}(\gamma') \approx \beta \, \mathrm{sgn}(\gamma), \qquad (6)$$

where we use γ instead of γ' for simplicity since the sign function is independent of the field strength but its direction. In the present study, the sign of J_{eff} is fixed, and hence the sign change of γ corresponds to the change in the direction of μ_z', which is experimentally possible. Accordingly, we choose the constant β to be negative to have a diamagnetic response to the magnetic field γ'.

III. CHERN NUMBERS AND EDGE CURRENT CHIRALITY

The total Hamiltonian for graphene in the presence of the exchange field is given by $H = H_{KMR} + H_{ex}$. For the bulk graphene, the Hamiltonian $H(\mathbf{k})$, which satisfies the periodicity $H(\mathbf{k}) = H(\mathbf{k} + \mathbf{G})$ ($\mathbf{G}$ stands for a 2D reciprocal-lattice vector), is given by

$$H(\mathbf{k}) = \begin{pmatrix} \lambda'\mathbb{Z} + \gamma & \mathbb{X} + i\mathbb{Y} & 0 & i\alpha\mathbb{M}_- \\ \mathbb{X} - i\mathbb{Y} & -\lambda'\mathbb{Z} + \gamma & -i\alpha\mathbb{M}_+^* & 0 \\ 0 & i\alpha\mathbb{M}_+ & -\lambda''\mathbb{Z} - \gamma & \mathbb{X} + i\mathbb{Y} \\ -i\alpha\mathbb{M}_-^* & 0 & \mathbb{X} - i\mathbb{Y} & \lambda''\mathbb{Z} - \gamma \end{pmatrix}, \qquad (7)$$

where $\lambda' = \lambda + \beta\,\mathrm{sgn}(\gamma)$ and $\lambda'' = \lambda - \beta\,\mathrm{sgn}(\gamma)$. The state vector is represented by $\psi^\dagger = (c_{\mathbf{k}A\uparrow}^\dagger, c_{\mathbf{k}B\uparrow}^\dagger, c_{\mathbf{k}A\downarrow}^\dagger, c_{\mathbf{k}B\downarrow}^\dagger)$, where A and B denote the two different sublattice points in the unit cell, respectively, and the arrows represent the spin directions. The matrix elements are given by $\mathbb{X} = t[1 + 2\cos(k_x')\cos(3k_y')]$, $\mathbb{Y} = t[2\cos(k_x')\sin(3k_y')]$, $\mathbb{Z} = 2\sin(2k_x') - 4\sin(k_x')\cos(3k_y')$, $\mathbb{M}_+ = [-1 + 2\cos(k_x' - \frac{\pi}{3})\cos(3k_y')] + i[2\cos(k_x' - \frac{\pi}{3})\sin(3k_y')]$, and $\mathbb{M}_- = [-1 + 2\cos(k_x' + \frac{\pi}{3})\cos(3k_y')] + i[2\cos(k_x' + \frac{\pi}{3})\sin(3k_y')]$, where the two variables k_x' and k_y' are defined as $k_x' \equiv \frac{\sqrt{3}}{2}k_x a$ and $k_y' \equiv \frac{k_y}{2}a$, respectively. Note that along the $k_y = 0$ profile, the two points $k_x' = \pm\frac{2\pi}{3}$ are just the K and K' points in the Brillouin zone of bulk graphene [see Fig. 1(c)], respectively. After the eigenvalue equation $H(\mathbf{k})|\psi_{n\mathbf{k}}\rangle = E_{n\mathbf{k}}|\psi_{n\mathbf{k}}\rangle$ is solved, the Berry curvature $(\Omega_{xy}^{(n)})$ of the nth band can be calculated using

$$\Omega_{xy}^{(n)}(\mathbf{k}) = -\sum_{n'(\neq n)} \frac{2\,\mathrm{Im}\langle\psi_{n\mathbf{k}}|v_x|\psi_{n'\mathbf{k}}\rangle\langle\psi_{n'\mathbf{k}}|v_y|\psi_{n\mathbf{k}}\rangle}{(E_{n'\mathbf{k}} - E_{n\mathbf{k}})^2}. \qquad (8)$$

The Chern number is then obtained by summing the Berry curvatures $\Omega_{xy}^{(n)}$ for all the occupied states below the Fermi level for each $\mathbf{k}$ and subsequently integrating over the entire first Brillouin zone:

$$\nu = \frac{1}{2\pi}\sum_n \int_{BZ} dk_x dk_y \Omega_{xy}^{(n)}(\mathbf{k}). \qquad (9)$$

The bulk Hamiltonian (7) is simplified greatly if we consider the following simple systems: (1) Kane-Mele system, $H_{KM} = H_t + H_\lambda + H_\gamma$, (2) Rashba system, $H_R = H_t + H_\alpha + H_\gamma$, and (3) Haldane system, $H_H = H_t + H_\beta + H_\gamma$. The sign
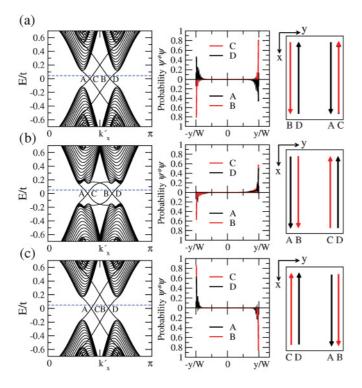
FIG. 2. (Color online) Calculated energy bands (left panels), edge state probability (middle panels), and charge current (right panels) distributions in the zigzag ribbon in the presence of the exchange field. The Fermi level (the dashed line in the left panels) $E_F = 0.05t$. (a) Kane-Mele system ($\lambda = 0.06t$ and $\gamma = 0.2t$). (b) Rashba system ($\alpha = 0.2t$ and $\gamma = 0.2t$). (c) Haldane system ($\beta = -0.07t$ and $\gamma = 0.2t$).

of Chern number indicates the chirality of the edge current. To verify the occurrence of the edge currents, we compute the energy band structure for a zigzag graphene ribbon. The unit cell of the zigzag graphene ribbon is shown in Fig. 1(a), where the ribbon direction is denoted by the x axis and the transverse direction is along the y direction. The width of the zigzag ribbon (W) is $75\,a$, where $a = 1.42$ Å[44] is the bond length [see Fig. 1(b)], i.e., there are $N + 1 = 101$ C atoms in the transverse direction [see Fig. 1(a)]. The nearest-neighbor hopping integral $t \approx 2.5$ eV.[44]

Figure 2 shows the ribbon band structure and the edge state probability distribution in the Kane-Mele system (a), the Rashba system (b), and the Haldane system (c). The Fermi level is assumed to be above zero, as indicated by the dashed horizontal line, and thus has four intersections with the conduction bands, denoted as A, B, C, and D, in the left panels in Fig. 2. This gives rise to four edge currents on the ribbon edges, as indicated by the A, B, C, and D arrows in the right panels in Fig. 2. The direction of an edge current, denoted by an arrow, is given by $I = -|e|v_x$ where the electron group velocity is determined using $v_x = \partial E_{\mathbf{k}}/\partial k_x$. The A and B states have the same velocity direction, which is opposite to that of the C and D states. Hereafter, we use the notation (I_L, I_R) to express the charge current distributions on the left-hand and right-hand side edges, respectively. In terms of the bulk-boundary correspondence, for each of the three systems, the pair A and D would form a single handed

loop (the turning point is at infinity in the x direction), and the pair B and C would constitute the other loop of the opposite handedness, as can be seen from the probability distribution shown in the middle panels in Fig. 2.

In the Kane-Mele system H_{KM}, the current distribution is (I_{BD}, I_{AC}), as indicated in the right panel in Fig. 2(a). The two edge states A and C are on the same edge, and so are the B and D states. As mentioned above, the handedness of the current loop due to the A and D edge states would produce a Chern number of -1 while that of the pair B and C would give a Chern number of $+1$. Therefore the Kane-Mele system is composed of two integer quantum Hall subsystems, namely, $(\nu = +1) \oplus (\nu = -1)$,[20,45] and has $\nu = (+1) + (-1) = 0$. Since this state has the same distribution of the edge currents as that of the quantum spin Hall case with the TRS,[20] except that the TRS is broken here, we call this state as the pseudoquantum spin Hall state (see Appendix A).

In the Rashba system H_R, the current distribution is (I_{AB}, I_{CD}), as shown in Fig. 2(b), which constitute a paramagnetic response to the exchange field. Both I_A and I_B are located at the same edge, confirming that the Rashba system has a Chern number of $+2$, since the two edge current pairs have the same chirality.[34] It is important to note that both the Chern number and the current distribution (I_{AB}, I_{CD}) in the Rashba system is invariant under the transformation $\alpha \rightarrow -\alpha$. On the other hand, the current distribution becomes (I_{CD}, I_{AB}) when the direction of the exchange field is reversed. Therefore, the Rashba system is equivalent to two integer quantum Hall subsystems, namely, $(\nu = +1) \oplus (\nu = +1)$ for $\gamma > 0$ or $(\nu = -1) \oplus (\nu = -1)$ for $\gamma < 0$.[34]

In the Haldane system H_H, the current distribution is (I_{CD}, I_{AB}), as shown in Fig. 2(c). Both I_A and I_B are also located at the same edge, but the chirality of the edge current is opposite to that of the Rashba system, as a result that the Haldane system with $\beta < 0$ exhibits a diamagnetic response to γ'. The Chern number of this system is $\nu = -2$. Therefore the Haldane system, being diamagnetic, is equivalent to two integer quantum Hall subsystems, namely, $(\nu = -1) \oplus (\nu = -1)$ for $\gamma > 0$ or $(\nu = +1) \oplus (\nu = +1)$ for $\gamma < 0$.

In the next two sections, we will consider the following two combinations of the three simple systems discussed in this section: (1) Kane-Mele-Rashba system: $H_1 = H_{KMR} + H_\gamma$ and (2) Haldane-Rashba system: $H_2 = H_t + H_\beta + H_\alpha + H_\gamma$. We find that, because of the bulk gap-closing phenomena, both systems will undergo a change of the edge current chirality caused by varying the exchange field.

IV. PHASE TRANSITION IN THE KANE-MELE-RASHBA SYSTEM

In this section, we will neglect the Haldane orbital coupling term of Eq. (5b). We will find that the phase transition is different from the QSH phase transition in the presence of the exchange field. We consider the interplay between H_γ and H_{KMR}:

$$H_1 = H_{KMR} + H_\gamma = H_t + H_\alpha + H_\lambda + H_\gamma. \quad (10)$$

In the presence of both Kane-Mele and Rashba spin-orbit couplings, the phase transition between the chiral (or antichiral) state and the pseudo-QSH state must occur when the bulk

gap-closing phenomena take place. On the other hand, although the locations of four currents (I_{BD}, I_{AC}) become (I_{AC}, I_{BD}) under the transformation $\lambda \to -\lambda$, the phase transition between (anti-) chiral and pseudo-QSH states still applies because both I_{BD} and I_{AC} correspond to $\nu = 0$.

In order to verify the phase transition in the finite system (the graphene ribbon), we use the expectation value of position y (i.e., $\langle y \rangle$) as a parameter for specifying the angular momentum of the current in the system, and define $\langle y \rangle = \langle y \rangle_A + \langle y \rangle_B$. When the Kane-Mele coupling λ is dominant ($|\gamma| < \gamma^c$, see below), $\langle y \rangle_A$ and $\langle y \rangle_B$ are on the opposite sides of the ribbon, and thus $\langle y \rangle / W = 0$. When the Rashba coupling is dominant ($|\gamma| > \gamma^c$, see below), $\langle y \rangle_A$ and $\langle y \rangle_B$ are on the same side of the ribbon. The quantity $\langle y \rangle / W$ in the Rashba dominant system, however, would not reach a saturated value $\langle y \rangle / W = \pm 1$ owing to the finite-size effect as the perfect edge states are obtained only when the ribbon width W is infinite. During the phase transition, the wave functions start to mix with each other in the central region of the ribbon, and thus $\langle y \rangle$ is expected to deviate from either 0 or ± 1.

In the Kane-Mele-Rashba system, the presence of λ and α would result in the asymmetry of conduction and valance bands. When we use the condition $\lambda > \alpha$, the band-touching point would be at zero energy. Furthermore, in order to compare the Kane-Mele-Rashba with the Haldane-Rashba system in the variation of Chern number, the order of magnitude of λ is numerically chosen as the same as that of α [see also Eq. (11) below]. Let us consider the case of $\lambda = 0.06t$, $\alpha = 0.05t$,[46] and γ ranging from $-0.5t$ to $0.5t$ in Eq. (10), as an example. (For the case of $\lambda = 0.006t$ and $\alpha = 0.005t$, see Appendix B). For $\gamma > 0$, we find that $\langle y \rangle$ decreases to zero near some magnitude of γ (see below) and does not change sign, as shown in Fig. 3(a). The pattern of $\langle y \rangle$ in the $\gamma < 0$ region is the parity symmetry of that in $\gamma > 0$. We find that the expectation value $\langle y \rangle$ changes sign when the direction of the chiral current is reversed.

Based on the bulk-boundary correspondence,[14,19] the existence of the phase transition is supported by evaluating the critical values of the exchange field. The critical value of the exchange field (γ^c) for the occurrence of the phase transition is determined by the bulk gap-closing phenomena, where the bottom of the bulk conduction band (E_c) and the top of the bulk valence band (E_v) become degenerate, namely, $E_c - E_v = 0$ at γ^c. It can be shown that the degenerate point is located at $k'_x = \pm \frac{2\pi}{3}$. The critical value for the exchange field is given by

$$\gamma^c = \pm \left(\frac{-\sqrt{3}\alpha^2 + 12\sqrt{3}\lambda^2}{4\lambda} \right), \tag{11}$$

which is obtained for a nonzero Kane-Mele coupling that satisfies $\alpha/\lambda < \sqrt{3}$. The presence of λ causes the critical value for the exchange field to shift from $\gamma^c = 0$ (Rashba system) to a nonzero value. The magnitude γ^c corresponds to the location where the bulk valence and conduction bands become degenerate and the Chern number starts to jump from one integer to another.

For a system with given α and λ, if $\gamma > \gamma^c$ ($\gamma < \gamma^c$), the system is in the chiral current state (pseudo-QSH state, see Appendix A). When $\gamma = +|\gamma^c|$ (or $\gamma = -|\gamma^c|$), the conduc-
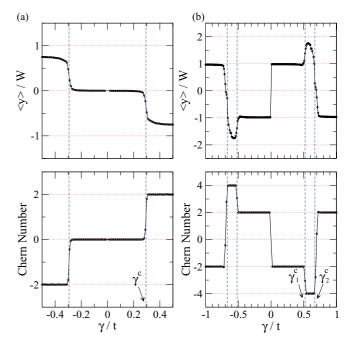

FIG. 3. (Color online) Expectation value $\langle y \rangle$ and Chern number as a function of γ/t. (a) The Kane-Mele-Rashba system with $\lambda = 0.06t$, $\alpha = 0.05t$, and γ ranging from $-0.5t$ to $0.5t$. (b) The Haldane-Rashba system with $\beta = -0.1t$, $\alpha = 0.5t$, and γ ranging from $-t$ to t.

tion and valance bands touch at $k'_x = 2\pi/3$ and $k'_x = -2\pi/3$ simultaneously. Because the I_A current direction is opposite to I_D, the exchange of the locations of I_A and I_D results in a change of chirality [see Fig. 3(a)]. The corresponding variation of the Chern number is also shown in Fig. 3(a). Therefore we find that the Chern number jumps from $\nu = 0$ to $\nu = \pm 2$. In this case, the critical values $\gamma^c = \pm 0.293t$ are in agreement with the numerical result.

V. PHASE TRANSITION IN THE HALDANE-RASHBA SYSTEM

In this section, we will neglect the Kane-Mele coupling λ. We will show that the presence of the Hamiltonian H_β creates two new edge modes between the two $\nu = \pm 2$ phases. Interestingly, these intermediate states are either the hyperchiral ($\nu = +4$) or antihyperchiral ($\nu = -4$) states. The Hamiltonian is given by

$$H_2 = H_t + H_\alpha + H_\beta + H_\gamma. \tag{12}$$

As described in Sec. III, the Haldane system has $\nu = -2$ and the Rashba system has $\nu = +2$ when the exchange field is positive. If the phase transition occurs in this system, the bulk gap-closing phenomena must take place. In the following, we show that the Haldane-Rashba system has two critical values of the exchange field.

For the sake of discussion, we consider the region with $\gamma > 0$, and focus on the region $k'_x > 0$ because the behavior of the corresponding degenerate points in $k'_x < 0$ is the mirror symmetry of that in $k'_x > 0$. In the presence of α only, there

are two degenerate points. One is at $k'_{x1} = 2\pi/3$ (i.e., K point), and the other is at

$$k'_{x2} = \cos^{-1}\left(\frac{2\alpha^2 - 1}{2\alpha^2 + 2}\right). \tag{13}$$

Equation (13) shows that the degenerate point depends on the strength of the coupling and thus varies with the magnitude of α. However, the two degenerate points appear simultaneously, namely, there is only one critical value for the exchange field, $\gamma^c = 0$, even when the coupling λ is considered [as shown in Fig. 3(a)].

Unlike the Kane-Mele coupling λ, we find that the coupling β will close the bulk gap *twice* at two different magnitudes of the exchange field. Namely, there are two degenerate points appearing at two different magnitudes of the exchange field. Therefore the Chern number varies discontinuously from $\nu = +2$ to $\nu = -2$ through an intermediate state. One of the degenerate points is at the K point; the corresponding critical value of the exchange field is

$$\gamma^c_1 = -3\sqrt{3}\beta, \quad k'^c_{x1} = 2\pi/3. \tag{14}$$

However, the second degenerate point for the Hamiltonian (12) is different from k'_{x2} expressed in Eq. (13). The second degenerate point is determined by the condition $E_v - E_c = 0$ and can be expressed as

$$\gamma^c_2 = -4\sqrt{3}\beta(1 - F^2), \quad k'^c_{x2} = \cos^{-1}(F), \tag{15}$$

where F satisfies the following equation:

$$-1 + 2\alpha^2 + 32\beta^2(1 - F^2 + F^3) - 2F(1 + \alpha^2 + 16\beta^2) = 0. \tag{16}$$

Numerically, Eq. (16) can be solved for a given set of α and β. When $\beta = 0$, Eq. (13) is the solution of Eq. (16), and the critical value of the exchange field is $\gamma^c_1 = \gamma^c_2 = 0$, which is in agreement with that in the case of the Rashba system. For the present case, $\alpha = 0.5t$ and $\beta = -0.1t$. The two critical points are $\gamma^c_1 = 0.5196t$ and $\gamma^c_2 = 0.68995t$. Therefore the conduction and valence bands first touch at $\gamma = \gamma^c_1$, and the bulk gap would reopen when $\gamma^c_1 < \gamma < \gamma^c_2$ (referred to as the intermediate state). The two bands would touch the second time at $\gamma = \gamma^c_2$. The bulk gap is open when $\gamma > \gamma^c_2$. The calculated Chern number as a function of γ/t is shown in Fig. 3(b).

Surprisingly, the intermediate state between the critical values γ^c_1 and γ^c_2 shows $\nu = -4$. The band structure and current distribution of the intermediate state are shown in Fig. 4. We find that in the presence of Haldane orbital effect, the system establishes two new edge modes: one is the pair A_2 and D_2, and the other is the pair C_2 and B_2. Furthermore, the current distribution I_L (and I_R) also shows that the four currents in I_L have the same chirality. Importantly, we find that unlike the quantum Hall plateau, the Chern number is not restricted in changing from one integer ν to the next integer $\nu \pm 1$. Instead, a higher Chern number can exist in a system with a spin-orbit interaction if the orbital effect is also taken into account.

The Chern number [see Eq. (9)] can be written as $\nu = \int_{BZ} dk'_x dk'_y \tilde{\Omega}_{xy}$. The bulk band structure and the corresponding Berry curvature $\tilde{\Omega}_{xy}$ along the $k_y = 0$ profile are shown
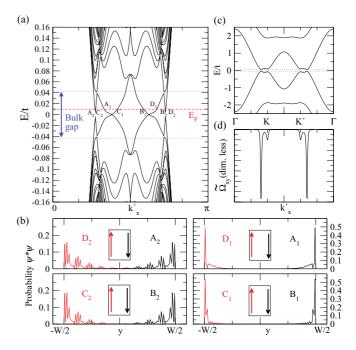

FIG. 4. (Color online) The band structure (a), the edge state probability and current distributions (b), bulk energy bands (c), and Berry curvature (d) of the intermediate state in $\gamma^c_1 < \gamma < \gamma^c_2$ ($\alpha = 0.5t$, $\beta = -0.1t$, and $\gamma = 0.6t$) (see text) in the graphene ribbon. The Fermi level E_F is at $0.01t$ [the red dashed line in (a)]. In (a), the eight edge states are marked as A, B, C, D, A_2, B_2, C_2, and D_2, respectively. In (c) and (d), the bulk energy bands and Berry curvature are plotted along the $k_y = 0$ profile.

in Fig. 4(c) and 4(d), respectively, where we use $\alpha = 0.5t$, $\beta = 0.1t$, and $\gamma = 0.6t$. It can be shown that if the linear term $\beta_1\gamma'$ is taken into account, the Chern number is still -4. This clearly shows that the anomalous Chern number $\nu = -4$ is due to the second nearest-neighbor hopping in graphene. We believe that if the third nearest-neighbor hopping is considered in Haldane orbital effect and spin-orbit interaction, a higher Chern integer of, e.g., -6, may be obtained.

Let us define $\langle y \rangle = \langle y \rangle_{A_1} + \langle y \rangle_{B_1} + \langle y \rangle_{A_2} + \langle y \rangle_{B_2}$ for the intermediate state. The calculated variation of $\langle y \rangle$ with γ is shown in Fig. 3(b). Apart from the occurrence of the intermediate state, the expectation value $\langle y \rangle = \langle y \rangle_A + \langle y \rangle_B$ changes sign as the exchange field is swept through the phase transition, and this is accompanied by a change of the Chern number from $\nu = +2$ to $\nu = -2$, as shown in Fig. 3(b).

The Chern number obtained from the bulk Hamiltonian represents the number of the perfect edge states. Note, however, that because of the finite-size effect, $\langle y \rangle/W$ cannot reach the saturated value $\langle y \rangle/W = \pm 2$ [see Fig. 3(b)]. Interestingly, we find that it is not necessary to reverse the direction of the exchange field in order to flip the current chirality in this case. Therefore the graphene can be brought to either the paramagnetic phase or the diamagnetic phase by adjusting the magnitude of the exchange field.

Very recently, Tse *et al.*[47] also proposed that the Hall conductance can be quantized as $\sigma_{xy} = 4e^2/h$, *albeit*, in bilayer graphene with the Rahsba coupling under the influence of an external gate voltage. In the present work, in contrast, we show that in single-layer grapnene, the quantized Hall

conductance can be $\sigma_{xy} = 4e^2/h$ when the Haldane orbital effect is considered. Furthermore, we find that the change in the quantized Hall conductance can be achieved by varying the exchange field instead.

Equations (14), (15), and (16) indicate that even when both α and β have very small but nonzero values, the bulk gap can also close twice at two different magnitudes of the exchange field. However, if they are order of $0.01t$, the width showing Chern number 4 would be $0.0003t$ and the energy gap is about $0.0001t$, which is very small in comparison with room temperature (0.025 eV $\sim 0.011t$). On the other hand, if both the Rashba and Haldane orbital couplings can achieve $0.1t$, the energy gap would be of the order $0.01t$ as shown in Fig. 4(a), which is experimentally detectable. Hopefully, our interesting prediction would stimulate measurements of the Chern number in such spin-orbit coupled system in the near future.

VI. CONCLUSIONS

In summary, we find that the edge current chirality in a graphene ribbon can be flipped by varying the exchange field. The resultant phase transition of the current chirality is caused by the bulk gap-closing phenomena; that is, the phase transition is due to the topological effect of the bulk band structure of graphene. We show that the paramagnetic response in the Rashba system can exhibit ether the chiral or antichiral state, and thus the Hall conductance is quantized as $\sigma_{xy} = \pm 2e^2/h$. We find that the Kane-Mele system has the pseudo-QSH state. For the Kane-Mele-Rashba system, the transition between the

chiral (or antichiral) current state and the pseudo-QSH state can be achieved by varying the strength of the exchange field.

Unlike the Rashba system, the Haldane system exhibits a diamagnetic response to the exchange field, and the quantized Hall conductivity is $\sigma_{xy} = \pm 2e^2/h$. However, the competition between α and β leads to a phase transition between the diamagnetic and paramagnetic responses, and hence an intermediate phase. Interestingly, this intermediate phase has two new edge modes and is thus a new quantum anomalous Hall state with high Chern number $\nu = \pm 4$. The corresponding quantized Hall conductance is $\sigma_{xy} = \pm 4e^2/h$ in the graphene ribbon in the absence of Landau levels.

APPENDIX A: PSEUDOQUANTUM SPIN HALL STATE

In this appendix, we numerically calculate the spin polarizations of edge states B and D in graphene ribbon with the Kane-Mele and Rashba couplings. Edge states B and D have different current chiralities. If they are located at the same edge, the corresponding Chern number of the bulk system is zero ($\nu = 0$). We call the state with $\nu = 0$ as the pseudo-QSH state
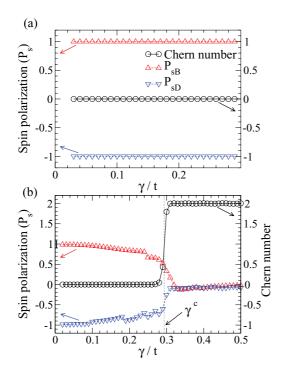

FIG. 5. (Color online) Calculated spin polarizations of edge states B and D in a graphene ribbon with (a) the Kane-Mele Hamiltonian ($\lambda = 0.06t$) and (b) the Kane-Mele-Rashba Hamiltonian ($\lambda = 0.06t, \alpha = 0.05t$).
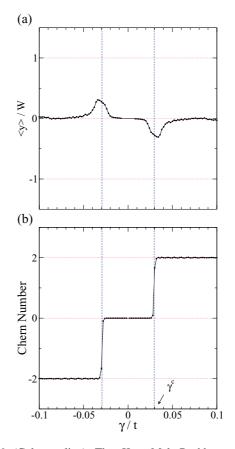

FIG. 6. (Color online) The Kane-Mele-Rashba system $\lambda = 0.006t$ and $\alpha = 0.005t$. The critical field is $\gamma^c = 0.0293t$. (a) The expectation value $\langle y \rangle$ and (b) the variation of Chern number.

in the sense that the spin polarization direction of B is always opposite to that of D. In the Kane-Mele and Kane-Mele Rashba systems, we will show that in zero-Chern-number regime both systems stay in the pseudo-QSH state.

The degree of spin polarization P_s of each edge state is defined as $P_s = P_+ - P_-$, where P_+ (P_-) is the sum of all spin-up (spin-down) probability through the graphene ribbon in y direction. We also have $P_+ + P_- = 1$ because the wave function is normalized.

In the Kane-Mele system, a small applied exchange field would open the band gap and the Chern number can be obtained. In this case, the Chern number is always zero and no phase transition occurs. As shown in Fig. 5(a), the degree of spin polarization of state B (P_{sB}) is the same as that of D (P_{sD}) when the system is in zero-Chern-number regime. We also have $P_{sB} = -P_{sD} = 1$. Namely, spin polarization of B is opposite to that of D in direction and the degree of spin polarization is 100% in both edge states.

In the Kane-Mele-Rashba system, the phase transition between $\nu = 0$ and $\nu = 2$ occurs at a nonzero exchange field. As shown in Fig. 5(b), in the zero-Chern-number regime, even though we have $|P_{sB}| \neq |P_{sD}|$, the spin polarization of state B is still opposite to that of D in direction.

APPENDIX B: CHERN NUMBER FOR SMALL COUPLINGS λ AND α

In this appendix, we calculate the Chern number and expectation value of $\langle y \rangle$ in the Kane-Mele-Rashba system by using $\lambda = 0.006t$ and $\alpha = 0.005t$, which are ten times smaller than the corresponding values in Sec. IV. We find that the Chern number still shows jumps from 0 to Ó2 as the absolute value of γ/t increases [see Fig. 6(b)]. The critical field $\gamma^c = 0.0293t$ can be obtained by using Eq. (11).

In this case, nonetheless, the energy gap becomes smaller than the case described in Sec. IV, being $0.012t$, which is still close to the room temperature. As a result, the predicted quantum phase transitions could perhaps be observed only at low temperatures. We also find that in this case, the edge states become rather delocalized and extend significantly into the central region of the ribbon (finite-size effect), such that the expectation value $\langle y \rangle$ is rather small [see Fig. 6]. The smallness of the calculated $\langle y \rangle$ could be partially attributed to the finite size (only 101 C atoms) of the ribbon width W used in the present calculation. Nonetheless, this suggests that in order to observe edge states experimentally, λ and α values should be larger than 0.005t.

*twchen@phys.ntu.edu.tw

†gyguo@phys.ntu.edu.tw

[1] K. S. Novoselov, A. K. Geim, S. V. Morozov, D. Jiang, M. I. Katsnelson, I. V. Grigorieva, S. V. Dubonos, and A. A. Firsov, Nature (London) **438**, 197 (2005).

[2] Y. Zhang, Y.-W. Tan, H. L. Stormer, and P. Kim, Nature (London) **438**, 201 (2005).

[3] V. P. Gusynin and S. G. Sharapov, Phys. Rev. Lett. **95**, 146801 (2005).

[4] V. P. Gusynin and S. G. Sharapov, Phys. Rev. B **73**, 245411 (2006).

[5] N. M. R. Peres, F. Guinea, and A. H. Castro Neto, Phys. Rev. B **73**, 125411 (2006).

[6] K. v. Klitzing, G. Dorda, and M. Pepper, Phys. Rev. Lett. **45**, 494 (1980); *The Quantum Hall Effect*, edited by R. E. Prange and S. M. Girvin (Springer-Verlag, Berlin, 1990).

[7] K. S. Novoselov, E. McCann, S. V. Morozov, V. I. Falko, M. I. Katsnelson, U. Zeitler, D. Jiang, F. Schedin, and A. K. Geim, Nat. Phys. **2**, 177 (2006).

[8] E. McCann and V. I. Falko, Phys. Rev. Lett. **96**, 086805 (2006).

[9] M. Nakamura, L. Hirasawa, and K.-I. Imura, Phys. Rev. B **78**, 033403 (2008).

[10] P. Lauffer, K. V. Emtsev, R. Graupner, Th. Seyller, L. Ley, S. A. Reshanov, and H. B. Weber, Phys. Rev. B **77**, 155426 (2008); Z. Liu, K. Suenaga, P. J. F. Harris, and S. Iijima, Phys. Rev. Lett. **102**, 015501 (2009); L. B. Biedermann, M. L. Bolen, M. A. Capano, D. Zemlyanov, and R. G. Reifenberger, Phys. Rev. B **79**, 125411 (2009); W. Norimatsu and M. Kusunoki, *ibid.* **81**, 161410(R) (2010); J. Borysiuk, J. Soltys, and J. Piechota, J. Appl. Phys. **109**, 093523 (2011).

[11] Y.-F. Hsu and G.-Y. Guo, Phys. Rev. B **82**, 165404 (2010).

[12] R. B. Laughlin, Phys. Rev. B **23**, 5632 (1981).

[13] B. I. Halperin, Phys. Rev. B **25**, 2185 (1982).

[14] D. J. Thouless, M. Kohmoto, M. P. Nightingale, and M. den Nijs, Phys. Rev. Lett. **49**, 405 (1982); D. J. Thouless, *Topological Quantum Numbers in Nonrelativistic Physics* (World Scientific, Singapore, 1998).

[15] R. Jackiw and C. Rebbi, Phys. Rev. D **13**, 3398 (1976); R. Jackiw, *ibid.* **29**, 2375 (1984).

[16] E. Fradkin, E. Dagotto, and D. Boyanovsky, Phys. Rev. Lett. **57**, 2967 (1986).

[17] F. D. M. Haldane, Phys. Rev. Lett. **61**, 2015 (1988).

[18] Y. Hatsugai, Phys. Rev. Lett. **71**, 3697 (1993).

[19] M. Z. Hasan and C. L. Kane, Rev. Mod. Phys. **82**, 3045 (2010).

[20] C. L. Kane and E. J. Mele, Phys. Rev. Lett. **95**, 226801 (2005).

[21] C. L. Kane and E. J. Mele, Phys. Rev. Lett. **95**, 146802 (2005).

[22] B. A. Bernevig and S.-C. Zhang, Phys. Rev. Lett. **96**, 106802 (2006); B. A. Bernevig, T. L. Hughes, and S.-C. Zhang, Science **314**, 1757 (2006); M. König, H. Buhmann, L. W. Molenkamp, T. Hughes, C.-X. Liu, X.-L. Qi, and S.-C. Zhang, J. Phys. Soc. Jpn. **77**, 031007 (2008).

[23] J. E. Moore and L. Balents, Phys. Rev. B **75**, 121306 (2007).

[24] L. Fu, C. L. Kane, and E. J. Mele, Phys. Rev. Lett. **98**, 106803 (2007); L. Fu and C. L. Kane, Phys. Rev. B **76**, 045302 (2007).

[25] H. Zhang, C.-X. Liu, X.-L. Qi, X. Dai, Z. Fang, and S.-C. Zhang, Nat. Phys. **5**, 438 (2009).

[26] L. Sheng, D. N. Sheng, C. S. Ting, and F. D. M. Haldane, Phys. Rev. Lett. **95**, 136602 (2005); D. N. Sheng, Z. Y. Weng, L. Sheng, and F. D. M. Haldane, *ibid.* **97**, 036808 (2006).

[27] T. Fukui and Y. Hatsugai, Phys. Rev. B **75**, 121403(R) (2007).

[28] S. Murakami, New J. Phys. **9**, 356 (2007); **10**, 029802 (2008); S. Murakami and S.-I. Kuga, Phys. Rev. B **78**, 165313 (2008).

[29] Z. Wang, N. Hao, and P. Zhang, Phys. Rev. B **80**, 115420 (2009).

[30] J. C. Y. Teo and C. L. Kane, Phys. Rev. B **82**, 115120 (2010).

[31]J. S. Smart, *Effective Field Theories of Magnetism* (Saunders Company, Philadelphia, 1966); N. Majlis, *The Quantum Theory of Magnetism* (World Scientific, 2007).

[32]C.-X. Liu, X.-L. Qi, X. Dai, Z. Fang, and S.-C. Zhang, Phys. Rev. Lett. **101**, 146802 (2008).

[33]R. Yu, W. Zhang, H.-J. Zhang, S.-C. Zhang, X. Dai, and Z. Fang, Science **329**, 61 (2010).

[34]Z. Qiao, S. A. Yang, W. Feng, W.-K. Tse, J. Ding, Y. Yao, J. Wang, and Q. Niu, Phys. Rev. B **82**, 161414(R) (2010).

[35]D. Huertas-Hernando, F. Guinea, and A. Brataas, Phys. Rev. B **74**, 155426 (2006); H. Min, J. E. Hill, N. A. Sinitsyn, B. R. Sahu, L. Kleinman, and A. H. MacDonald, *ibid.* **74**, 165310 (2006); Y. Yao, F. Ye, X.-L. Qi, S.-C. Zhang, and Z. Fang, *ibid.* **75**, 041401(R) (2007); J. C. Boettger and S. B. Trickey, *ibid.* **75**, 121402(R) (2007).

[36]A. H. Castro Neto and F. Guinea, Phys. Rev. Lett. **103**, 026804 (2009).

[37]J. Zhou, Q. Liang, and J. Dong, Carbon **48**, 1405 (2010).

[38]A. Varykhalov, J. Sanchez-Barriga, A. M. Shikin, C. Biswas, E. Vescovo, A. Rybkin, D. Marchenko, and O. Rader, Phys. Rev. Lett. **101**, 157601 (2008).

[39]Y. S. Dedkov, M. Fonin, U. Rudiger, and C. Laubschat, Phys. Rev. Lett. **100**, 107602 (2008).

[40]N. M. R. Peres, F. Guinea and A. H. Castro Neto, Phys. Rev. B **72**, 174406 (2005).

[41]N. Tombros, C. Jozsa, M. Popinciuc, H. T. Jonkman, and B. J. van Wees, Nature (London) **448**, 571 (2007); H. Haugen, D. Huertas-Hernando, and A. Brataas, Phys. Rev. B **77**, 115406 (2008).

[42]Y. Wang, Y. Huang, Y. Song, X. Zhang, Y. Ma, J. Liang, and Y. Chen, Nano Lett. **9**, 220 (2009).

[43]H. S. S. Ramakrishna Matte, K. S. Subrahmanyam, and C. N. R. Rao, J. Phys. Chem. C **113**, 9982 (2009).

[44]A. H. Castro Neto, F. Guinea, N. M. R. Peres, K. S. Novoselov, and A. K. Geim, Rev. Mod. Phys. **81**, 109 (2009).

[45]X.-L. Qi, Y.-S. Wu, and S.-C. Zhang, Phys. Rev. B **74**, 085308 (2006).

[46]S. Murakami, Prog. Theor. Phys. Suppl. **176**, 279 (2008).

[47]W.-K. Tse, Z. Qiao, Y. Yao, A. H. MacDonald, and Q. Niu, Phys. Rev. B **83**, 155447 (2011).